The 14th International Topical Meeting on Nuclear Reactor Thermalhydraulics, NURETH-14
Toronto, Ontario, Canada, September 25-30, 2011

NURETH14-222

CFD Simulation on Flow Induced Vibrations in High Pressure Control and Emergency Stop Turbine Valve

H. Lindqvist[1]
[1] Forsmark Kraftverk AB, Östhammar, Sweden

Abstract

During the refuelling outage at Unit 2 of Forsmark NPP in 2009, the high pressure turbine valves were replaced. Three month after recommissioning, an oil pipe connected to one of the actuators was broken. Measurements showed high-frequency vibration levels. The pipe break was suspected to be an effect of highly increased vibrations caused by the new valve. In order to establish the origin of the vibrations, investigations by means of CFD-simulations were made. The simulations showed that the increased vibrations most likely stems from the open cavity that the valves centre consists of.

Introduction

During the outage of 2009 in unit 2 at Forsmark Nuclear Power plant, the Main Steam Stop-Control Valves (MSCV) where modified in context of the reactor upgrade to 120 % load. The housing of the valve was kept while the internal parts where replaced with a different design. Also, new actuators were installed. About three weeks after recommissioning, in December 2009, a pipe line to one of the actuators were detected to be broken. Extensive measurement revealed very high vibration levels in the steam lines and valves. Severe "hammer strokes" with accelerations over 50 g was also revealed in the measurements, see Figure 1. Frequency analysis of the vibrations showed levels up to 2 kHz.

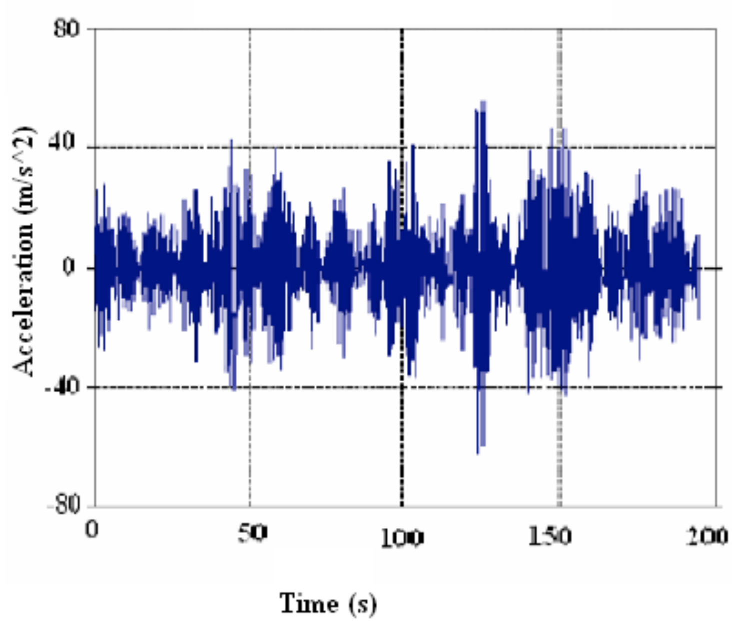

Figure 1 Forces on steam line after MSCV

These forces appeared repeatedly in the system and caused damages inside the valve, see Figure 2.

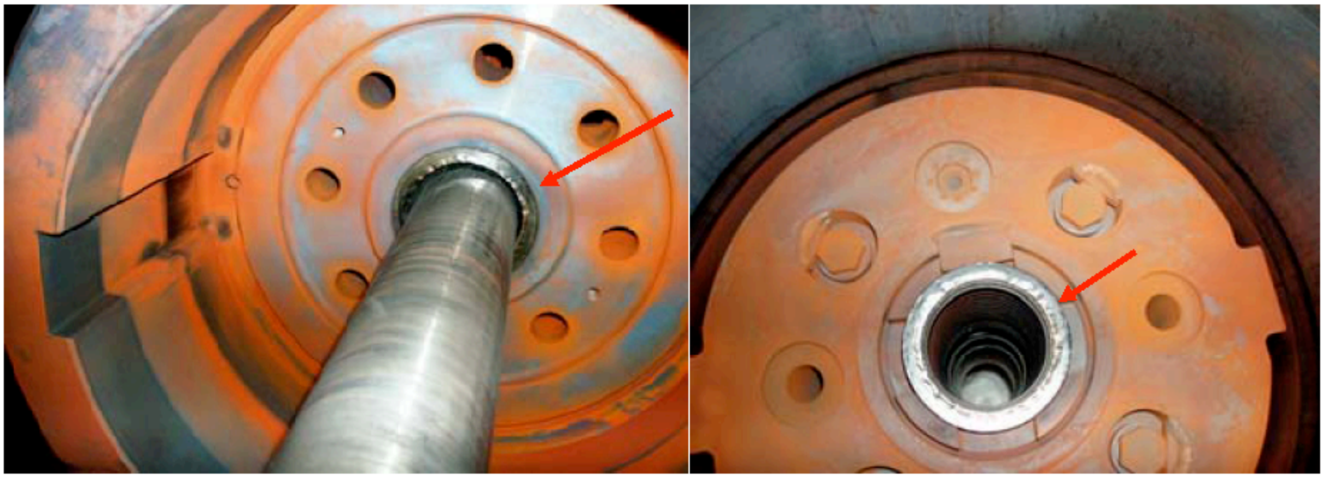

Figure 2 Damages on the stop valve. The site of damage shown with red arrows was located on the back side of valve cone (left) and at the seat above (right).

The "hammer strokes" was concluded to most likely originate from a strong irregularly flow field inside the valve, which periodically resulted in a very low static pressure in the centre of the valve. This very low static pressure pulled the valve cone downward, the cone accelerated back against its opening position when the pressure inside the valve increased. This impact was very hard. Observations of cracks on the valves foundation where also detected.

This paper presents results of Computational Fluid Dynamics (CFD) on the dynamic behavior of the flow field inside the valve. Simulations have been made with the software FLUENT 12.1, [1], on both the modified valve discussed above (hereby called the new valve) as well as the previously installed valve (hereby called original valve) for comparison. This has been done to verify the root cause of the extensively increased vibration levels on the steam lines that arose after the replacement. Calculations have been performed with 108 % reactor load, which is equal to a flow rate of 184 kg/s passing through each MSCV. One important aspect to mention about these simulations is that it has <u>not</u> been made to quantify any forces or vibration levels that the valves experienced. The objective of the project was to investigate and compare the velocity field inside and at the outlets for the two valves respectively and identify the root cause of the problem.

1. Valve design and geometrical appearance

Figure 3 shows a vertical cut of the new valve (left) and the original valve (right). The flow is going from bottom to top. A steam strainer precedes the inlet to the valves, which essentially is cylinder perforated with holes. This dampens a large part of the instabilities created by pipe bends, T-junctions etcetera, creating stable flow conditions before the flow enters the valve. The new valve features an open cavity at the centre of the valve, while the original valve has an annular gap formed by a centre body and the valve house wall.

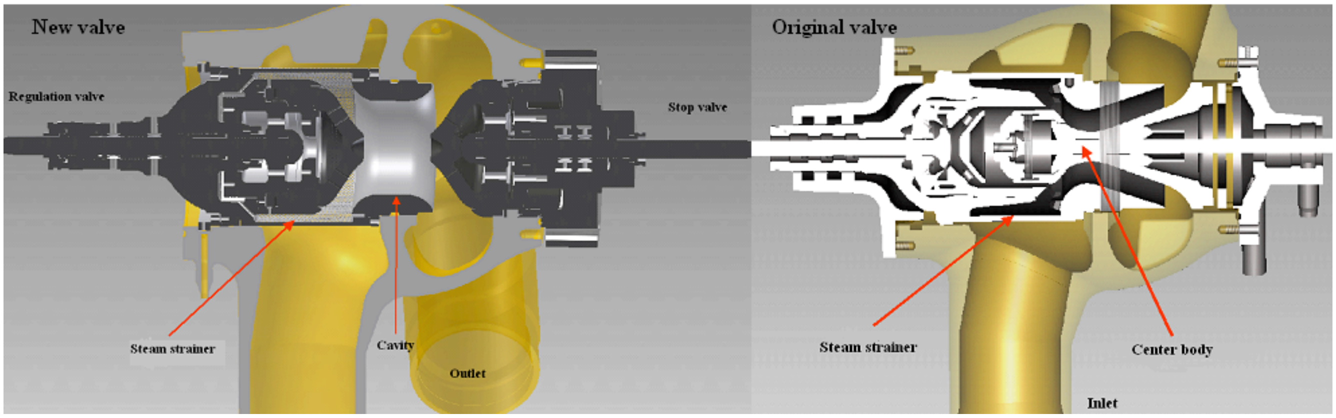

Figure 3 Vertical cut of the new valve, to the left, and the original valve, to the right

2. CFD modelling

2.1 Mesh description for the original valve

The mesh generated for the original valve consisted of 16.1 million tetrahedral elements, see Figure 4. It has a maximal aspect ratio of 187 and a maximal skewness of 0.96. This is below the recommendation of maximal skewness in [1]. The mesh has a fairly equal distribution through out the model but is less dense at the inlet part, which is not shown in Figure 4. The mesh size was chosen to be the maximum affordable for the computer used.

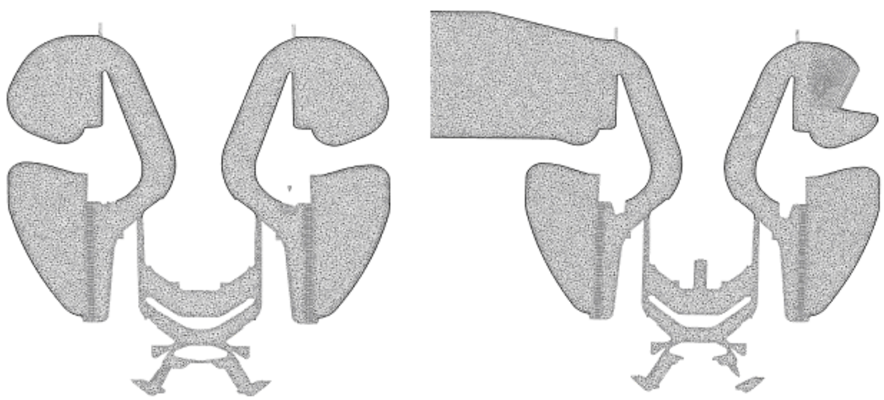

Figure 4 Vertical cut showing cell distribution

2.2 Mesh description for the new valve

The mesh generated for the new valve was non-conformal, consisting of a 9.6 million mixture of hexahedral and tetrahedral elements as shown in Figure 5, the mesh was provided by the vendor. Most of the elements are hexahedral. Max aspect ratio was 34.6 with a maximum skewness of 0.94. Figure 5 shows that the mesh density was concentrated to the centre part of the valve, where it also consisted only of hexahedral elements.

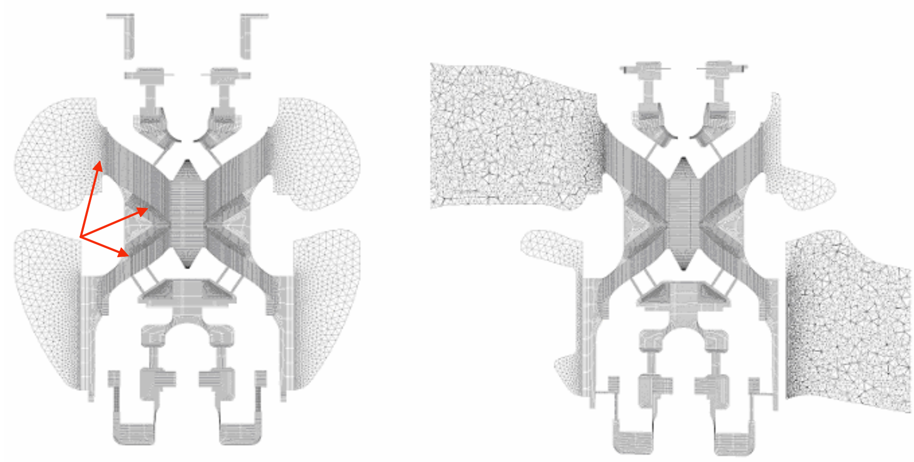

Figure 5 Vertical cut bisecting showing cell distribution

2.3 Turbulence model

The turbulent Reynolds Average Navier Stokes (RANS) models are based on the assumption that the flow field is steady in the mean. RANS-models are in its present form very dissipative, which means that medium to low turbulent scales are filtered. Unsteady RANS (URANS) is a time dependent simulation; the model is however still kept in the same manner as in a RANS calculation. Traditionally, the next step is a Large Eddie Simulation (LES). In a proper LES most of the turbulent scales are resolved, except for the very smallest, which are dissipated into heat. This put great demand on the computational power and requires a very fine mesh. A proper LES is in fact not applicable for most of the industrial flows today.

For these calculations, the SST-kω model developed by Menter [2] has been used. This model coalesce two known and well used two-equation models, k-ω and k-ε**.** The SST-model combines the careful formulation of the k-ω in the near wall regions with k-ε in the free stream with a blending function [3]. A User Defined Function (UDF) has been used to modify the turbulent viscosity in order to resolve more of the small scaled turbulent fluctuations. This approach to URANS modelling, called Partially Resolved Numerical Simulation (PRNS) or Very Large Eddy Simulation (VLES) is suggested by Liu & Shi (2006) [4]. It is motivated by the proposition that small scale turbulent motions are associated with small time scales and allows the use of a temporal filtering for defining the resolved scales. It has been demonstrated that temporal filtering seamless unites a URANS behavior of a simulation in some flow regions with the behavior of a LES in other regions [5].

2.3.1 <u>Description of VLES</u>

VLES is described in literature as an attempt to bridge the gap between URANS and LES. In a URANS simulation, most of the turbulence is modelled; in LES the large-scale turbulent structures are resolved in a fine mesh and the smallest non-resolved structures are modelled in what is referred to as a sub-grid model. In this contribution, temporal filtering of the Navier-Stokes equations is performed and the unresolved scales are accounted for by an eddy viscosity model. Depending on the temporal filter width, the dependent variables in the Navier-Stokes equation can evolve from a URANS to LES. The turbulent viscosity μ_t in the SST-kω model implemented by Fluent can be written as:

$$\mu_t^{VLES} = RCP\mu_t^{SST-k-\omega} \qquad (1)$$

The Resolution Control Parameter, RCP, in equation (1) is defined as the ratio of two time scales, the filter width and the global turbulent time integral scale. The lower limit of RCP may be obtained using the quota of length scales, which is also supported by [5] according to the analysis of [4]. To sum up the discussion above and conclude the effect of this modified description of the turbulent viscosity, the following can be said: A simulations acts as a pure URANS when RCP = 1, and act as a DNS when RCP $\rightarrow$ 0. In these simulations, the same value of RCP, 0.38, was used as in [4]. Also, smaller values of RCP were tested, but no improvement in the simulation could be detected. The first validation of this approach carried out by the present author was a participation of the OECD/NEA-vatenfall T-junction Benchmark experiment (8), (9), which showed good agreement with the experiment. Further validation on the approach is in progress, including also conjugated heat transfer.

2.4 Modelling the steam

The thermo dynamic properties of the steam are approximated with the theory of corresponding state, [6], with the following modified ideal gas law.

$$Z = \frac{Pv}{R_i T} \tag{2}$$

Z is the dimensionless compressibility factor, P is the absolute pressure [Pa], $v = \rho^{-1}$ is the specific volume [$\mathrm{m^3/kg}$], R_i is waters specific gas constant $461{,}527\,[\mathrm{J \cdot kg^{-1} \cdot K^{-1}}]$ and T is the temperature in [K].

For real gases as steam is $\mathrm{Z} \leq 1$ except for pressures and temperatures much higher than the critical values. FLUENT uses $Z \equiv 1$ as default, this means that the product $\left(Z \cdot R_i\right)$ must be altered to be able to model the thermo dynamical behavior of the steam [6].

The specific gas constant is in FLUENT $R_i = \mathbf{R}/M_i$, where $\mathbf{R} = 8.314510\ [\frac{\mathrm{J}}{\mathrm{mol \cdot K}}]$ is the universal mole gas constant and $\mathrm{M_i} = 18.0152\,[\mathrm{kg/kmol}]$ is the mole mass of water. It is necessary to change the mole mass of the water to adjust the specific gas constant with the aid of Z. The ideal gas approximation means however, that the specific heat at constant volume c_v and speed of sound, defined according to $\sqrt{\left(\mathrm{c_p R_i T}\right)/\left(\mathrm{c_p - R_i}\right)}\,[\mathrm{m/s}]$ do not correspond to values in [7] and gives an error in speed of sound of about 7 % and a few % in enthalpies. This means that applications such as heat transfer and pressure propagations are not suitable for this kind of approximation. This is however not the case here.

Table **1** specifies the thermo dynamical properties for steam at 65.3 bars, which was the operating condition for the simulations.

Pressure [Pa]	$65{,}3 \times 10^5$
Quality	1
Temperature [K]	554,3152
Z	0,754944
$(Z \cdot R_i)$ [J/kg·K]	348,4271
M_i [kg/kmol]	23,86299
Isobaric specific heat c_p [kJ/kg·K]	5,124085

Table 1Thermo dynamic properties for steam at 65.3 bar

2.5 Modelling the steam strainer

A steam strainer is preceding the inlet to the valves as mentioned before. The strainers function is mainly to smooth and reduce any arbitrary fluctuations in the flow caused by pipe bends, T-junctions etcetera. Figure 6 shows the position of the steam strainer for the new valve in the red box. The strainers position for the original valve is very much the same. There are about 20000 perforated holes at the strainers wall which the fluid goes through before entering the valve. This makes it almost impossible to model the strainer explicitly. Instead, it is modeled as a porous media, thereby allowing a pressure drop over the strainer. FLUENT specifies this with inertial losses [1]. For this case, the inertial resistance is 276, which is obtained from the vendor. The porosity of the strainer is 0.2 and these constants have been used for both models. The flow direction through the strainer is specified to the normal of the strainers surface.

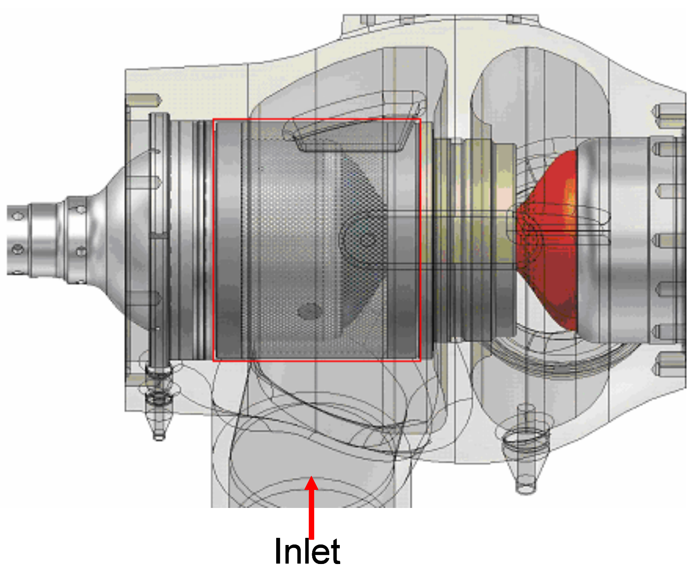

Figure 6 Steam strainers position in the new valve

2.6 Boundary condition, starting condition and time step

The boundary condition consists of mass flow rate of 184.375 kg/s for the inlet and an outlet vent was used at the outlet. The inlet temperature was 554 K used in both simulations. The time step was chosen so that a courant number sufficiently under 1 was achieved. A time step of 10^{-5} s was used which correspond to a courant number of 0.3-0.6 for the simulations. The calculated time was approximately 0.5 s. A transient quasi steady state was simulated for about 2 s, before starting sampling data. The passing through time for the flow was about 0.1 s, which mean that there was about 20 passes through the valve before sampling of data was started. This was considered to be sufficient to get rid of most of the initial conditions. The operating condition for the simulations was 65.3 bar.

3. Results

3.1 Simulations with the original valve

The shape and design of this valve is fairly basic and well composed, where a long, rather narrow channel guides the flow from the inlet to the outlet. During the simulation variables were monitored. 38 monitor points was taken inside and after the valve during the simulated time. The variable in question was velocity, pressure and temperature. Figure 7 shows number id, position and coordinate of some monitor points. In this paper, only velocities are presented because it is the fluctuating velocities that are the root cause to vibrations. The sampling frequency for the variables in each monitor point was taken every time step (10^{-5} s), that is 100 kHz.

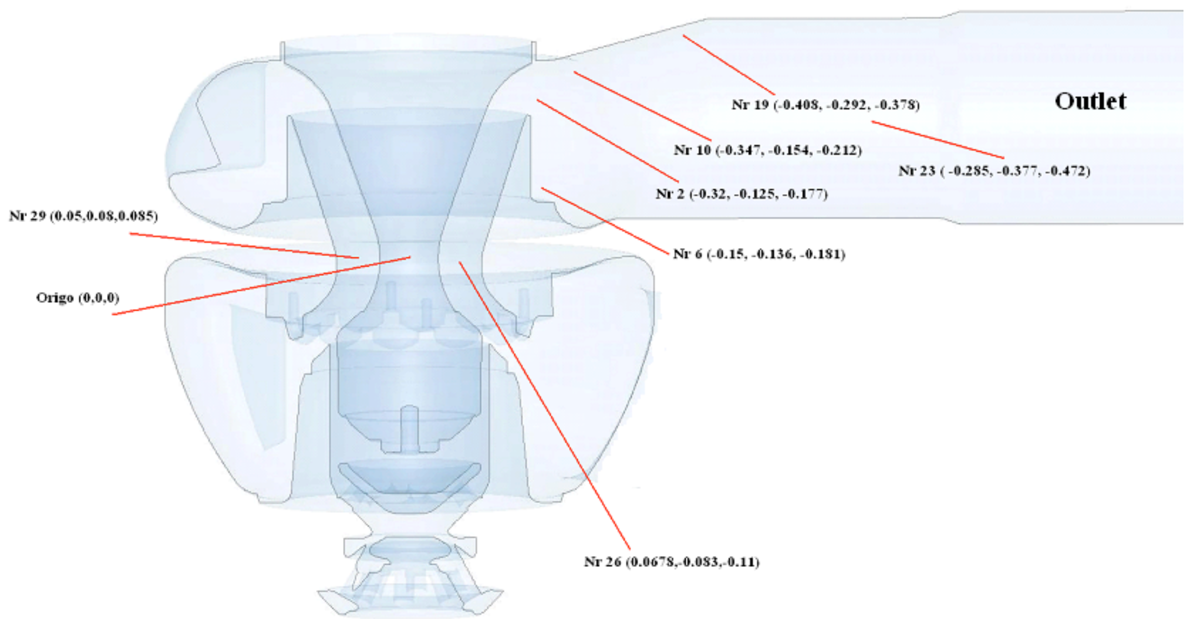

Figure 7 Number id: s, position and coordinates for the monitor points taken

Figure 8 shows a time sequence of velocity magnitude for the simulation with the original valve. The time sequence shows very stable flow conditions inside the valve, where the flow is guided in the annular gap without any significant fluctuations. As can be seen in the figures, there is an abrupt end to the outlet channel. This very abrupt end creates a strong separation, which pushes the flow up against the upper part of the outlet pipe, thereby creating stable conditions for the flow. There is however a zone with low velocities (around 20 m/s) that fluctuates back and forth in the middle of the outlet pipe. But, most important, the flow with high velocities is kept at the top of the pipe and in a stable manner.

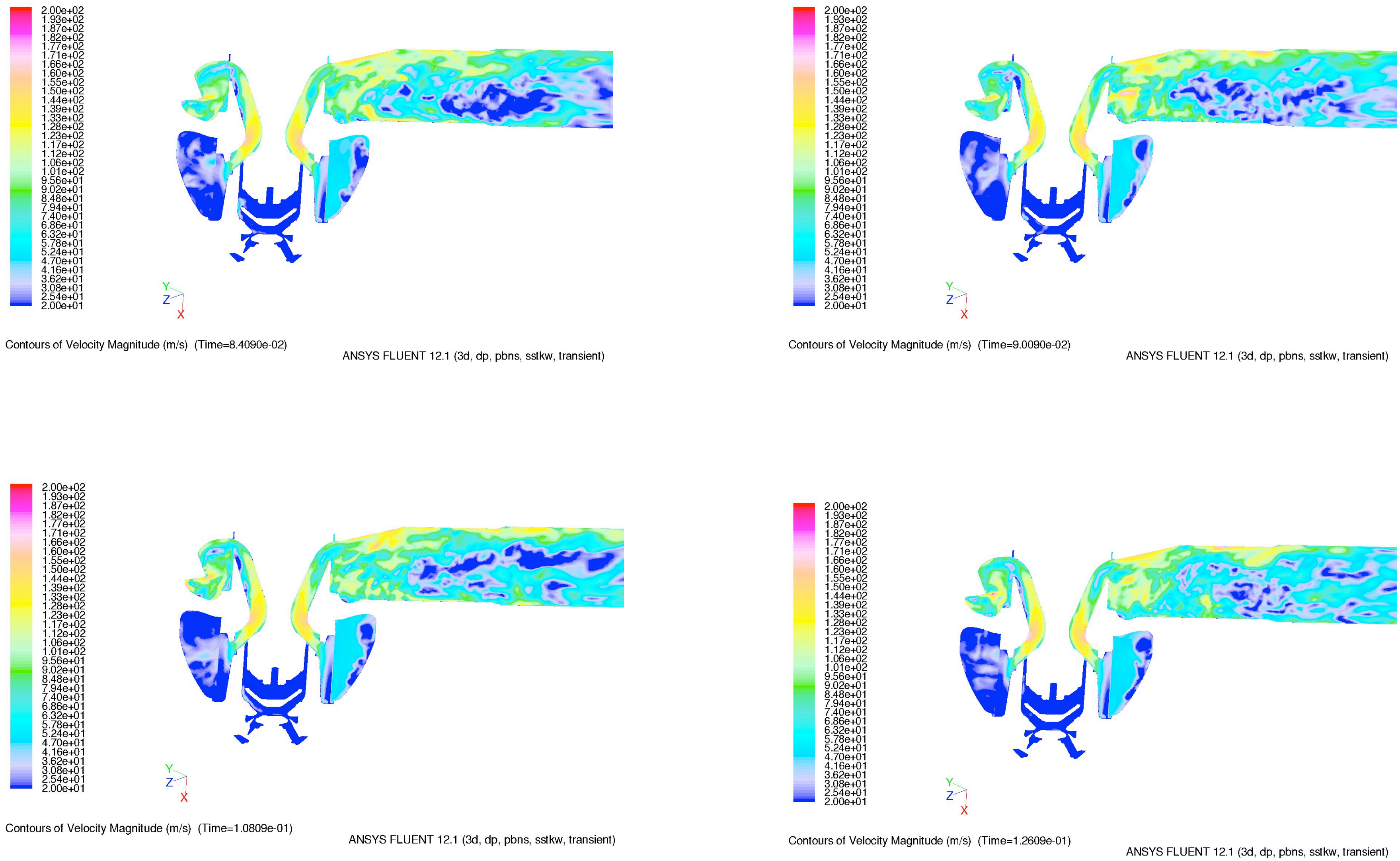

Figure 8 Vertical cut of the original valve bisecting origo showing a time series of velocity magnitude

Figure 9 shows velocities and frequency analysis for two monitor points, one inside the valve and the other at the outlet. Those two are characteristic for the monitor points in this simulation. There are very high velocities inside the valve. The simulation shows velocities up to 140 m/s. Still, there are very small fluctuations inside the valve. The picture is a little bit different for the outlet; the mean velocity is about 60 m/s, with quite strong fluctuations. Most of the energy in the signal lies in the lower part of the frequency band although there is quite high energy present up to 450 Hz.

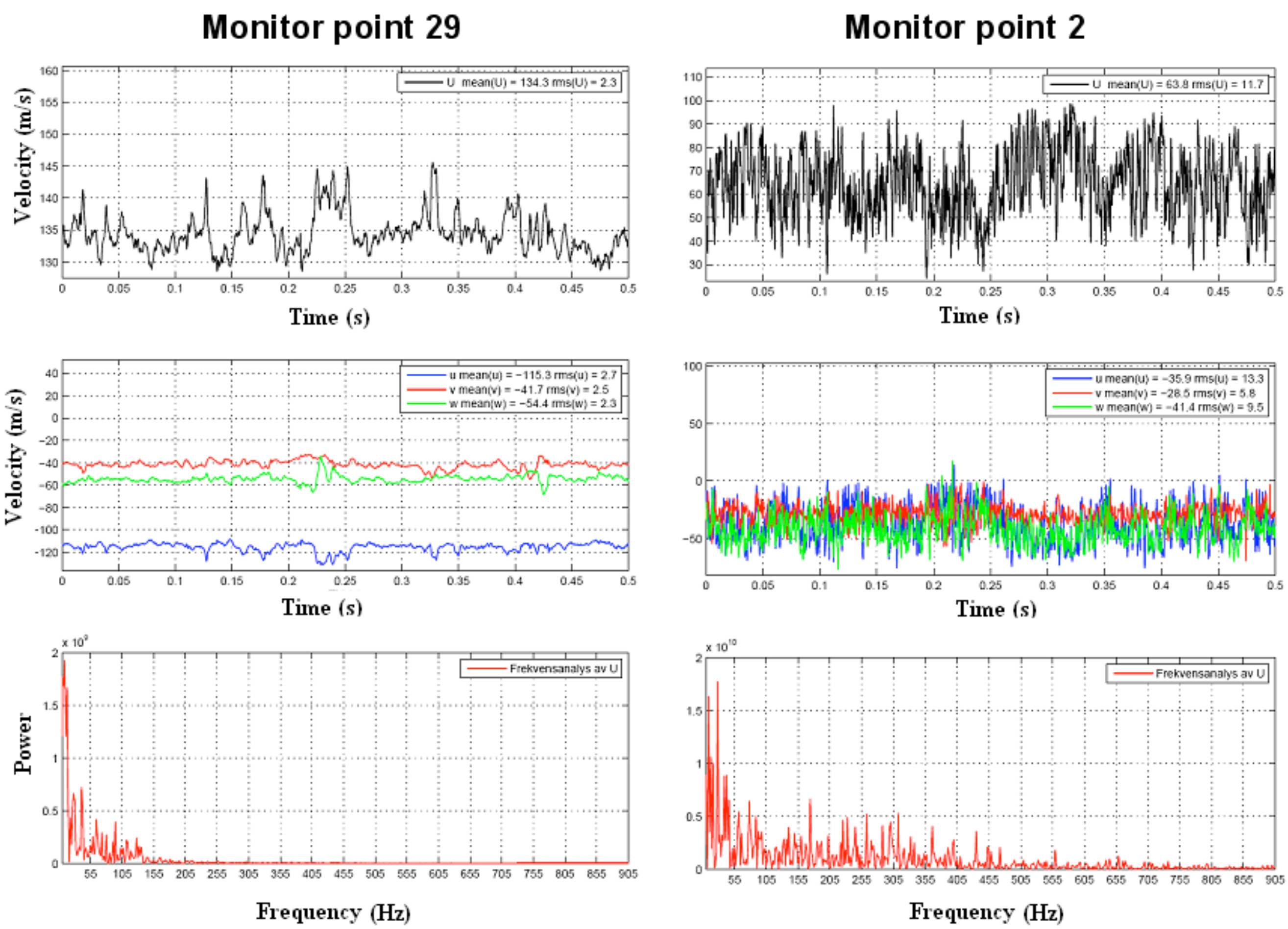

Figure 9 Velocities and frequency analysis for monitor point 2 and 29

3.2 Simulations with the new valve

147 monitor points where sampled with a sampling rate of 100 kHz in the simulation with the new valve. Figure 10 show some of the monitor point's with number id, position and coordinates.

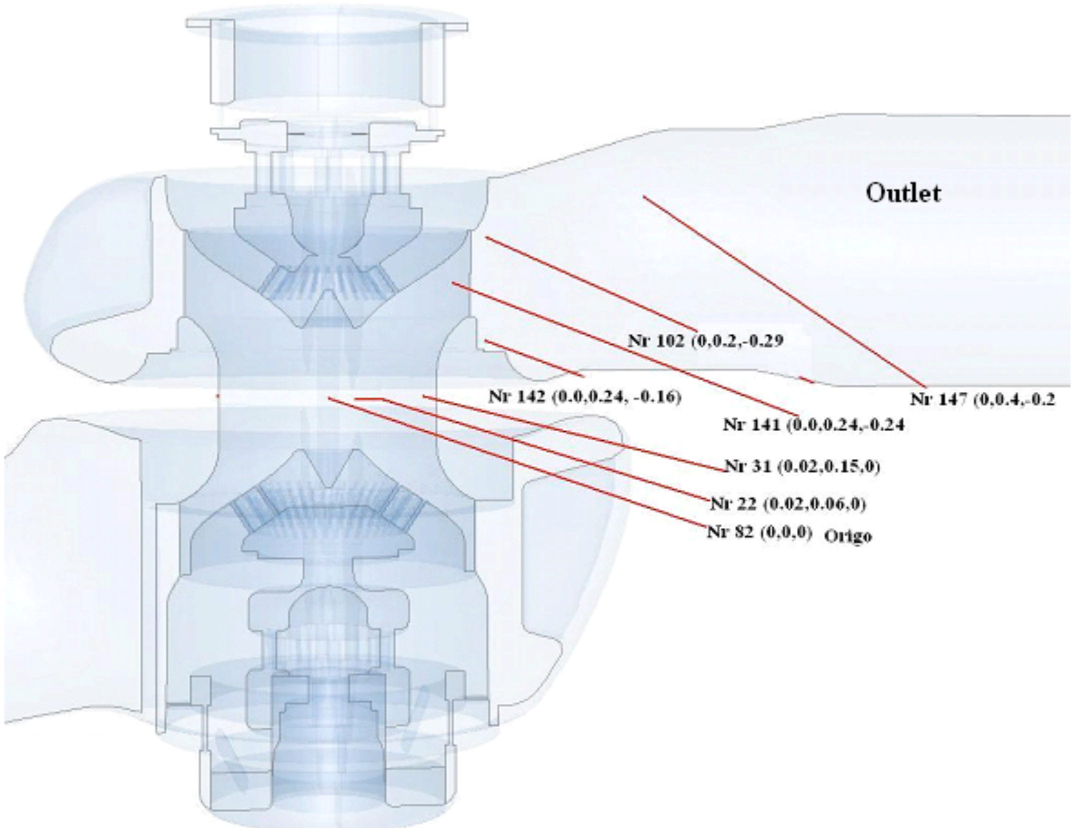

Figure 10 Number id: s, position and coordinates for the monitor points taken

Figure 11 showing a vertical cut bisecting origo with time sequences of velocity magnitude. The flow goes through the strainer, passes the regulation valve cone and enters the open cavity with a velocity around 130 – 140 m/s. Holes penetrates the regulation valve cone. The purpose was to dampen fluctuations in the centre of the valve according to the vendor. Figure 11 shows that there is a quite strong irregular separation from the second hole row at the cone that influence the flow pattern negatively (red line to the upper left in Figure 11). The steam enters to the centre of the valve with a high velocity, where it embodies a strong irregular velocity field.

The outlet of the valve is preceded by a short channel formed by the stop valve cone and the wall. This is not ideal considering instabilities for the outlet. Also, in the short channel a double separation appears. The flow separates from the wall and from the side of the stop valve cone, (brown lines to the lower left in Figure 11 points out the area). It is however not very clear in this time sequence, but the tendencies are there. The outlet conditions also show instable relations in the velocity field.

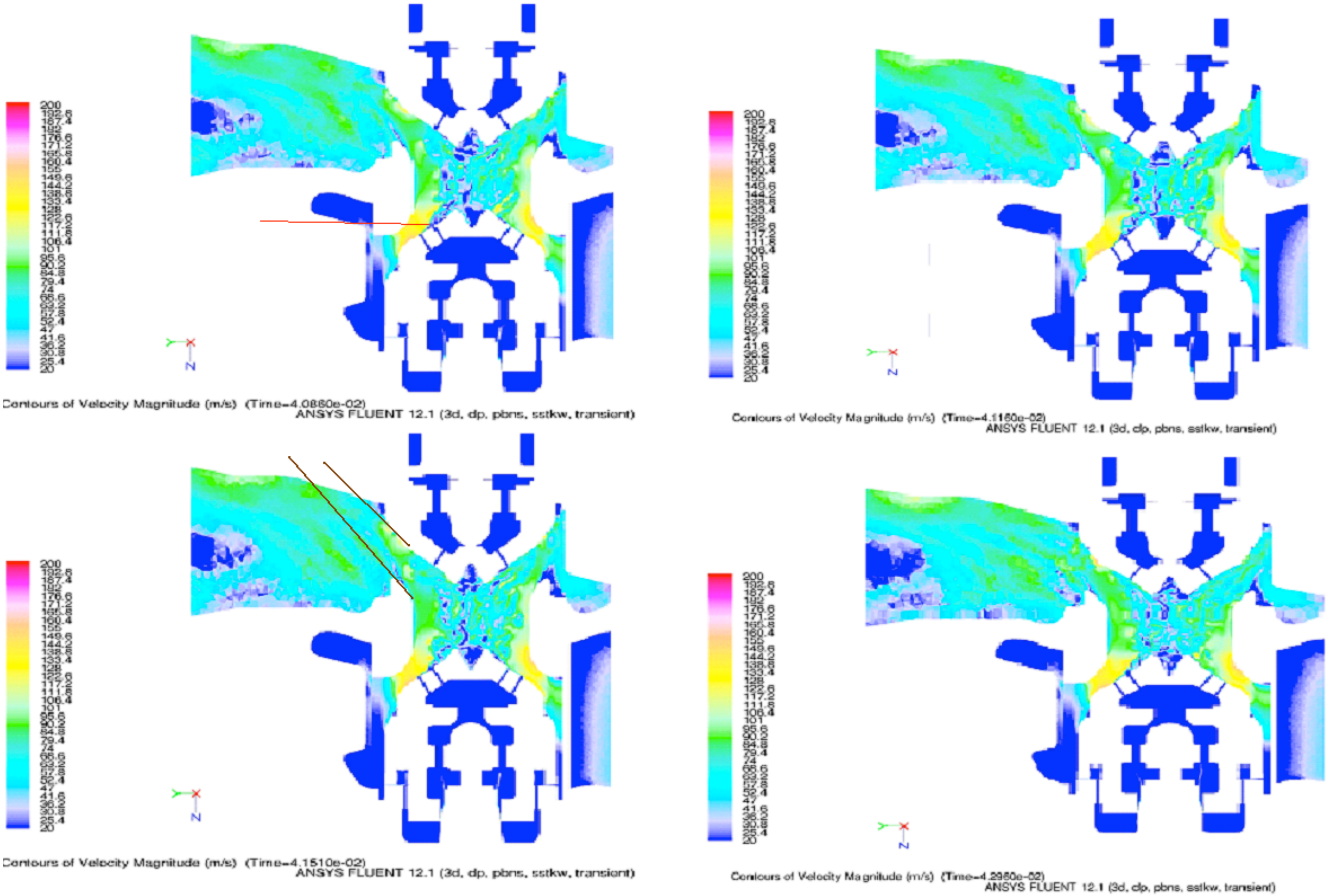

Figure 11 Vertical cut of the new valve bisecting origo showing a time series of velocity magnitude

Figure 12 shows two chosen monitor points, one inside and one at the outlet. There are strong fluctuations at the centre of the valve as can be seen from monitor point 22. The mean velocity is about 76 m/s, but fluctuates from 0 up to 140 m/s, within mille seconds. The very strong stochastic behaviour of the velocity field inside the valve creates high impulses on the walls, which most likely excites large amplitude vibration levels. The frequencies are dominant around 100 Hz, but there is also fairly high energy in the signal at about 320 Hz. There are also high impulses from the velocity fluctuations at the outlet, as can be seen in Figure 12. The energy in the frequencies lies within the bandwidth 350 – 600 Hz.

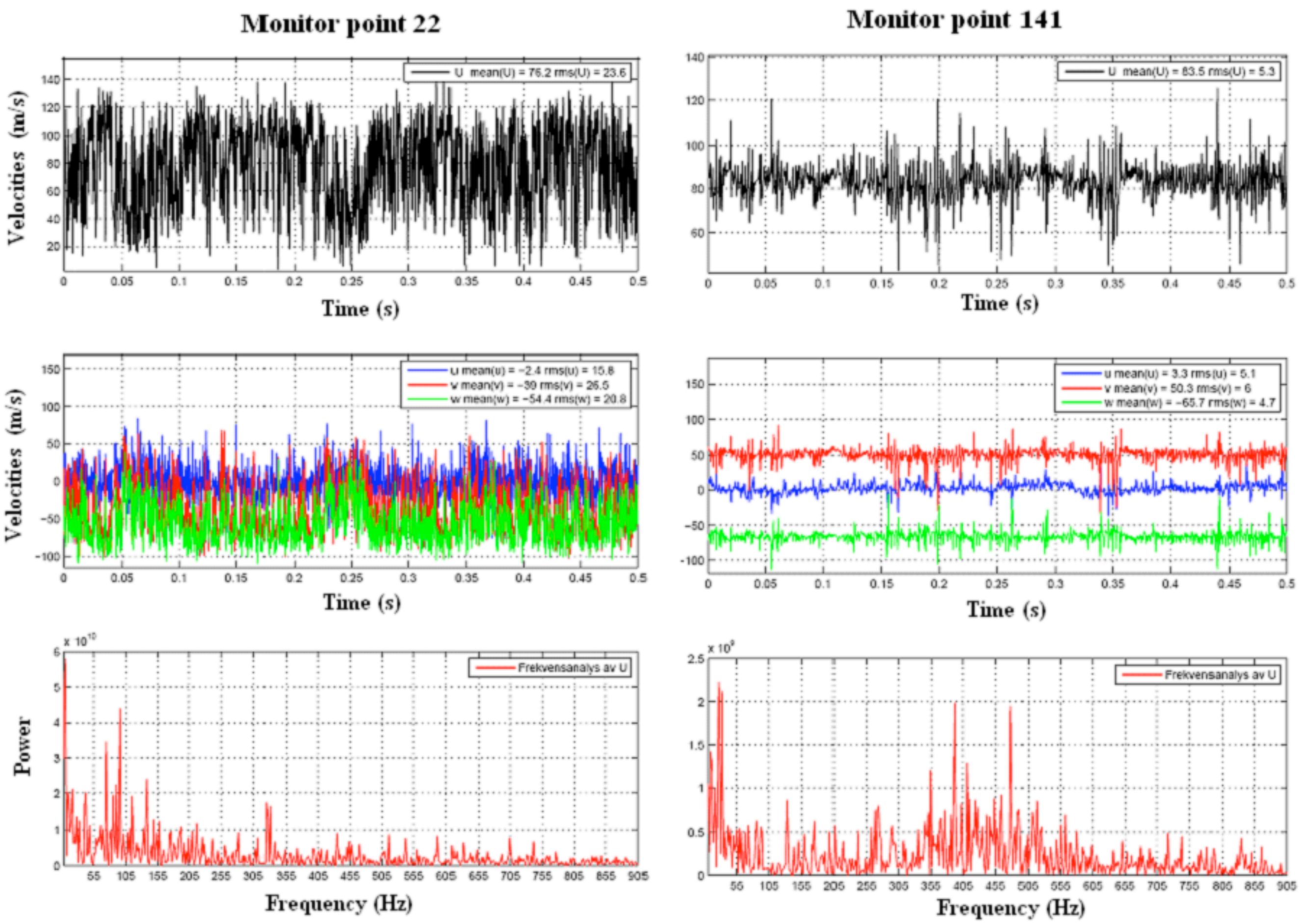

Figure 12 Velocities and frequency analysis for monitor point 22 and 141

3.3 Comparison of impulses

Figure 13 shows impulse per mass unit in a given point in the valves. This is of course not directly related to the force that the valve experience. The left plot in Figure 13 shows a comparison of the acceleration of the fluid at the centre of the valves and it is a huge different between the new and original valve. The differences are not as prominent at the outlet compared to the centre, but have very likely a great impact on the elevated vibrations levels experienced after the valve replacement.

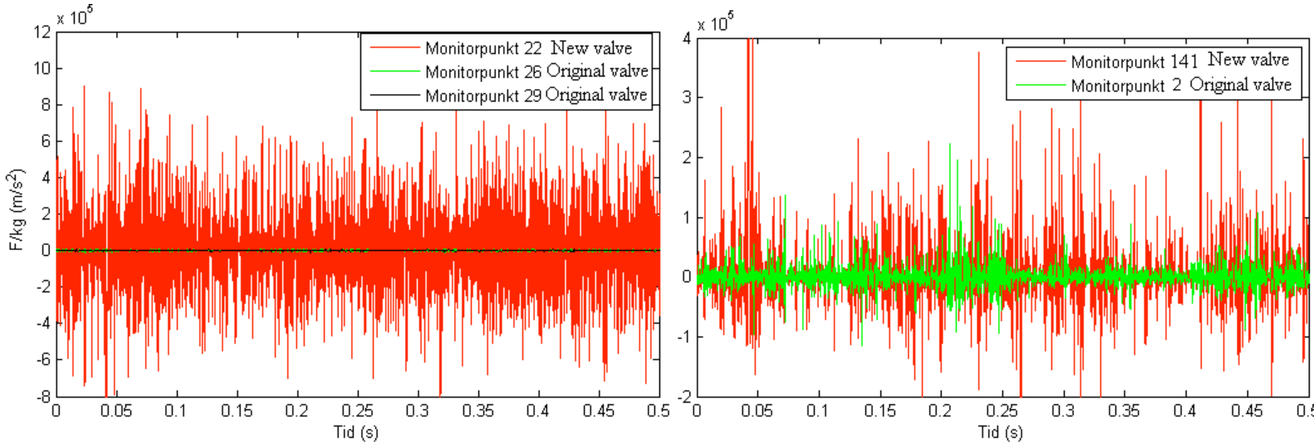

Figure 13 Impulse per mass unit at center of valve (left) and outlet (right)

4. Conclusions and discussion

Measurements made in the plant showed that the vibration levels increased enormously after the replacement. The simulations show that the root cause for the increased levels most likely stems from the open cavity that the new valves centre consist of. The flow actually merges or collides with very high velocity after been divided by the regulation valve cone, thus creating a strong stochastic fluctuating behaviour of the flow field. There are a couple of things besides the open cavity that probably further contributes to the vibrations. The simulation shows that there is a fluctuating separation from the regulation valve cone caused by the holes that penetrates the cone. A short channel formed by the wall and stop valve cone display a double stochastic separation of the flow. Also, the outlet exhibits strong fluctuations, which probably further increases the instabilities and contributes to the extensive vibrations.

5. References

[1]ANSYS FLUENT, “FLUENT 6.3 Documentation”, Fluent Inc., Lebanon, NH, 2006

[2] F. R. Menter, “Two-Equation Eddy-Viscosity Turbulence Models for Engineering Applications”, *AIAA Journal*, **32,** No. 8, pp.1598-1605, 1994

[3]Pope, S. B. (2000). “Turbulent Flows”, Cambridge University Press, ISBN 0-521-59886-9, UK.

[4] Liu, N. S. & Shih, T. H., (2006). “Turbulence Modeling for Very Large-Eddy Simulation”, AIAA Journal, Vol. 44, pp. 687-697

[5] Fadai-Ghotbi, A., Friess, C., Manceau, R., Gatski, T. B. & Borée, J. “Temporal Filtering: A Consistent Formalism for Seamless Hybrid RANS-LES Modelling in Inhomogeneous Turbulence”. Notes on Numerical Fluid Mechanics and Multidisciplinary Design, 2010, Volume 111/2010, 225-234, DOI: 10.1007/978-3-642-14168-3_19

[6] A. Bejan, “Advanced Engineering Thermodynamics”, John Wiley and Sons, New York, 1997

[7] E. Schmidt, and U. Grigull, “Properties of Water and Steam in SI-Units”, Springer-Verlag, Berlin, Germany, 1989

[8] OECD, (2010). "OECD/NEA-Vattenfall T-junction Benchmark Exercise: Thermal fatigue in a T-junction, CFD4NRS-3, Experimental Validation and Application of Computational Fluid Dynamics and Computational Multi-Fluid Dynamics Codes to Nuclear Reactor Safety Issues", OECD/NEA & IAEA Workshop hosted by USNRC, September 14-16 2010, Washington.